MRS Advances © 2018 Materials Research Society
DOI: 10.1557/adv.2018.399

Functional Materials through Surfaces and Interfaces[†]

Boyce Chang, Andrew Martin, Paul Gregory, Souvik Kundu, Chuanshen Du, Millicent Orondo, Martin Thuo*

Department of Materials Science and Engineering, Iowa State University, Ames, IA-50010, USA

[†]*presented at the 9th Conference of the African Materials Research Society, Gaborone, Botswana*

ABSTRACT

In most materials, surfaces and interfaces present a significant portion of the workable area, but this area has often been erroneously perceived as a challenge in processing and thus, largely ignored. Surfaces and interfaces, however, present a network of energetically mismatched (sometimes metastable) molecules that can be exploited to either control surface reactions, engineer bulk stability or reveal new fundamental details of otherwise not well understood processes or systems as described herein. This perspective captures the role of i) structure, ii) chemistry and iii) thermodynamics at the interface in fabricating functional materials. Engineering substrate morphology enables tunable wettability either through the substrate or an adsorbed self-assembled monolayer (SAM), the latter being largely due to effect of sub-nanoscale roughness on conformational defects and overall order in the SAM. Surface roughness and chemistry also dictates the nature and amount of adventitious contaminants on a surface, and this was used to control volume of adsorbed water leading to controlled and tunable step-growth polymerization. The chemical treatment renders the paper amphiphobic, which could be used for self-cleaning surfaces and nucleation of water microdroplets for water harvesting. Finally, creating a self-passivating polished thin (~0.7-2 nm) shell on a molten metal microdroplet kinetically frustrates solidification leading to significant undercooling. The ambient undercooled liquid metal is used for mechanically-triggered heat-free solder and smart composites. These three cases demonstrate key aspects of surface and interface engineering in integrating well-known concepts for the development of functional materials.

INTRODUCTION

"God made the bulk; surfaces were invented by the devil" —Wolfgang Pauli

Surfaces (the outermost part of any material)[1] and interfaces (a special type of surface forming a boundary between disparate components or phase that are part of a

larger system)[1] are abundant in materials and sometimes dictate a material's utility (function).[2] Surface atoms differs from its bulk counterpart in terms of energy, reactivity, dynamics, and occasionally composition.[2] They are often viewed as defects because of differences from bulk—hence the famous quote by Wolfgang Pauli.[3] This view has drastically changed as a myriad of applications such sensors[4, 5], MEMs and NEMs[6], lubricants[7], and hydrophobic surfaces[8] have been realized through in-depth understanding of these ubiquitous components of materials.

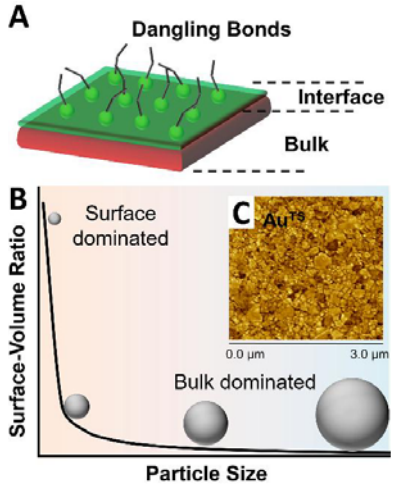

Figure 1. (A) Molecular structure at the surface of a material highlights transition to the bulk and presence of surface dangling bonds. (B) Surface area to volume ratio as a function of particle size, illustrating the dominance of surfaces at smaller length scales. (C) Interfaces present in template stripped polycrystalline gold surface. The actual interfacial surface area available is estimated to be ~12x larger than the apparent 3x3 µm section (Reprinted with permission from Langmuir 32, 10358 (2016). Copyright (2018) American Chemical Society).[9]

Scientific definition of surfaces and interfaces is an on-going debate largely due to the paradox embedded in their existence; i.e., establishing equilibrium between two units of significantly different chemical potential that are in contact. Existence of such an equilibrium state violates the zeroth law of thermodynamics. To overcome this paradox, interfaces are either made up of equilibrium-dictated concentration gradients (Gibbs interfaces)[10] or metastable states.[11, 12] Presence of coordinative hypo-valency or dangling bonds (Figure 1A) provides an opportunity for surface engineering through chemisorption or physisorption. This unique type of bonds translates to surfaces being an active reaction front that can be selectively targeted without any consequences to the bulk. Chemisorption of hydrocarbons (for example multi-functional silanes), is among the most commonly used method for engineering surfaces.[13, 14] A general negligence of physisorbed adventitious adsorbates and their underlying structures (e.g. bound water) have limited, and sometimes misinformed, our interpretation of the structure of chemisorbed reagents.[15, 16] We recently demonstrated that adventitious contaminant could participate in surface reactions and should be an integral component of the design process.[17] In some cases, however, a strong adsorbate-substrate bond may overcome

any detrimental effects on the produced adsorbed layer albeit with effect on the assembly kinetics.[18]

Another interesting feature regarding interfaces is their thermodynamic environment. In liquids, continuous relaxation and/or diffusion into the bulk results in an active system.[10] The transient and divided nature of the interface, complicates the location of such a boundary. They are typically modelled using the Gibbs dividing surface[10], whereby concentration gradients are created to passivate energy mismatch between distinct phases induced by lattice mismatch and differences in chemical potential. Such gradients create built-in potential difference, which induces a pseudo-equilibrium. From a reaction perspective, this poses a problem as this potential acts as a kinetic barrier separating the reactants. Most notable examples include passivating oxide layers on metal surfaces[19] and p-n junctions[20] in semiconductors. These built-in potential differences at the surface are sufficiently large in microscale particles due to high surface area to volume ratio (Figure 1B), and has been deployed to stabilize metastable states in metals.[21] The significance of interfaces can also be seen when comparing total interfacial surface area of polycrystalline materials with their apparent sectional surface area, for example on a polycrystalline gold surface (Figure 1C)[22] the former is *ca.* 12x larger than the latter.

Spontaneous surface reactivity is also responsible for generation of passivating layers on reactive systems like metal alloys. Inherent differences in reduction potentials, stoichiometry, and reaction kinetics under various processing conditions, however, renders the passivating layer a complex micro- or nano-system.[23, 24] Asymmetry in reactivity of components making up a liquid metal alloy leads to the establishment of concentration gradients while stoichiometric imbalance, and subsequent vacation of the eutectoid global energy minima, may lead to interface phase-segregation of the less reactive component in its pure form.[25-27] Consequences of the concentration gradients and concomitant underlying reaction driven segregation of a metallic thin film of the less reactive component(s) dictates that such a system would create an ultra-smooth self-assembled high chemical potential interface. We inferred that such a structural and energetically complex interface can; i) eliminate heterogeneous nucleates, ii) offers an opportunity to manage energetics in the bulk and could introduce new capabilities in processing of metallic alloys.

Surfaces and interfaces, thus, have large potential for creating functional materials. Heterogeneity in composition and nanoscale texture, however, substantially influence apparent surface tension/energy. To engineer surfaces as functional material platforms, it is essential to revisit fundamental aspects governing structure-property relations. It has been shown that surface roughness, and molecular orientation affects surface energy.[22, 28, 29] Conflicts in this complex topic, most notably the Porter-Whitesides discrepancy[30], highlights the lack of understanding and the critical need for further development. Self-assembled monolayers (SAM) serve as an effective platform for studying the nature of such surfaces due to tenability in the molecular packing density, order, orientation, and structure of the SAM.

Herein, we summarize this effort into three aspects of interfaces, *viz*: i) Structure – we first demonstrate the importance of structural order in delineating wetting properties in n-alkanethiolate self-assembled monolayers (SAMs) on noble metal. This effort allowed us to unravel the Whitesides-Porter discrepancy as a surface roughness effect and point to the fundamental role of molecular orientation and sub-nanoscale roughness in tuning surface energy. ii) Chemistry – understanding chemical environment on an interface allows us to exploit adventitious bound water to engineer surface polymerization and gel formation on paper. Surface-energy mismatch drives self-assembly of the polymerizing fragments, leading to an amphiphobic material—that is, a material that has both hydrophobic and hydrophilic regions on its surface. iii)

Thermodynamics – driving bulk metastability through interfaces. Transitioning deeper into the surface, complexity in passivating oxide layers of metal surfaces enables us to create metastable liquid metal (undercooled), which we utilize for heat-free solders and smart composites.

FUNDAMENTALS OF SURFACES: STRUCTURE-PROPERTY RELATIONS IN SELF-ASSEMBLED MONOLAYERS

Self-assembled monolayers (SAM) have been broadly studied with respect to applications in tuning surface chemistry of materials. SAMs are widely used to fabricate well defined interfaces with applications such as sensors[4], molecular electronics[31], organic field-effect transistors[32], photovoltaic devices[33], liquid crystal alignment[32], biosensors[5], and lubricants.[7] There are basically two types of SAM; i) chemisorbed (covalently bonded on the surface), and ii) physisorbed (secondary bonds between molecule and substrate). Chemisorbed SAMs on smooth substrates are generally highly oriented due to packing and secondary interactions. Alkanethiol on gold(Au) and silver(Ag) substrates are the most widely studied and simplest form of SAMs from structural point of view. Effect of overall order and substrate morphology on surface energy (delineated via a liquid-SAM interface) can be understood by studying wetting behaviour using a library of probe liquids of known properties.[18] Besides the probe liquid, manifestation of interface structure due to the nature of the assembly and molecular parity, is best captured in the so-called odd-even effect. This odd-even oscillation in surface properties emanates from orientation of the terminal moiety assuming a defect free SAM.

(I) The Odd-Even Effect

The odd-even effect is widely observed in charge transport[31, 34], wetting[9, 22, 28, 29, 35], friction[36, 37], spectroscopy/microscopy[38-43], thermal properties[44, 45], mechanical properties[46], liquid crystal phases[45, 47, 48], among other properties. This effect is induced by changes in orientation of the SAM's terminal group (Figure 2A) as we alternate from odd to even numbered chains and vice versa. In an ideal SAM, this alternating orientation leads to changes in the orientation of dipole moments near the interface. From wetting studies, a difference in contact angle between the odd- and even-numbered homologs was observed.[29] This odd-even oscillation is not only structural, but also defect and substrate-roughness dependent.[9, 18, 22, 29, 35] It is therefore possible to engineer wettability of a surface through the molecule, substrate morphology, or terminal group.

(II) Effect of Surface Roughness

The odd-even effect is a manifestation of the structure of alkyl chains, which scales with the ordered nature of the SAMs. Thus, disruption of this order, by surface defects such as surface asperities, will perturb coherent molecular ordering of the SAM and in turn, at the very least, dampen empirical observation of the odd-even effect (Figure 2A). Felicitous choice of surface texture, however, has the potential to tune surface energy of the SAMs akin to the role of multi-level textures in superhydrophobic surfaces (example shown in Figure 2B). Roughness and chain-length dependent limits to observation of an odd-even effect were recently reported.[22, 29, 38] The odd-even effect in wetting properties of SAMs formed on silver surfaces (0.6 nm < R_{rms} < 2.5 nm) using various probe liquids (both wetting and non-wetting) empirically confirmed the

loci of the roughness limit.[22, 29, 38] Other surface parameters such as average grain area, surface coverage, power spectral density and bearing volume were also evaluated.[9] The static contact angles of different probe liquids (water, glycerol and hexadecane) showed a disappearing odd-even effect. Interestingly, only the totally wetting probe liquid (hexadecane) showed odd-even effects irrespective of substrate roughness. Observation of the odd-even effect in wetting with polar liquids (e.g. water and glycerol) show a dependency on substrate roughness, where the odd-even effect is observed only on smooth surface ($R_{rms} \leq 0.63 \pm 0.08$nm) but not on rough surface ($R_{rms} \geq 1.15 \pm 0.17$nm). This empirical evidence supports the idea that there is a roughness beyond which the odd-even effect cannot be observed, and the transition point was estimated at R_{rms} = 1 nm through extrapolation of wetting data. Besides being a useful tool in engineering wetting, we recently demonstrated that this wetting behaviour is an appropriate probe for SAM structure evolution where we demonstrated that various chain-length phase transitions occurs in agreement with a decrease in total gauche defects.[18, 35]

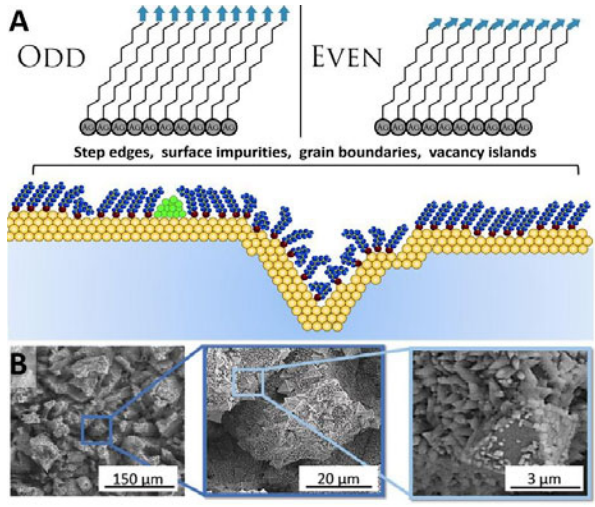

Figure 2. (A) Difference in orientation of the surface dipole moments with odd-even parity of hydrocarbon chain. Surface asperities and defects disrupts uniform packing of SAMs (Reprinted with permission from Journal of Physical Chemistry Letters 6, 4952 (2015). Copyright (2018) American Chemical Society).[49] (B) Multiscale and complex textures of copper which was primarily hydrophilic but eventually transformed into super-hydrophobic due to texturing (Reproduced from Nanoscale 8, 3982 (2016) with permission of The Royal Society of Chemistry).[50]

TUNING WETTABILITY: STEP-GROWTH POLYMERIZATION INDUCED SELF-ASSEMBLY (PISA)

The use of trifunctionalized alkylsilanes in synthesis of hydrophobic surfaces is widely reported, albeit with disparity on the underlying mechanism and/or products.[51, 52] When silanes are chemisorbed onto hydroxylated materials like cellulose, it is often inferred that a reaction between the surface hydroxyls and the silanes ensues, leading to a monolayer. We, [17] and others [15], have, however, shown that a different mechanism is involved. Oyola et. al. showed that presence of physisorbed water (Figure 3C) on a surface leads to step-growth polymerization between the silanes and water.[17] Where moiety valence is amenable to gel formation, tuning the amount of adsorbed water (limiting reagent) leads to self-assembled particle formation. Surface energy mismatch between the hydrocarbon tails of the silane and adsorbed water induces self-assembly of the oligomerized material leading to localization and formation of spherical particles. Kinetically controlled growth in the particles size leads to tunability in the ratio of hydrophobic-hydrophilic regions. The stochastic nature of the underlying surface reaction, coupled with asymmetry in the reactivity of the water molecules with respect to proximity to the surface, ensures that the polymeric particles attach randomly on the surface. This gives an averaged wettability where the new layer of roughness gives higher static water contact angles than expected based on surface chemistry equivalence (Teflon). Figure 3A-B show the comparison of the reaction processes. Figure 3D shows paper with particles formed on the surface of cellulose after silane treatment. The treated paper became superhydrophobic with contact angles greater than the chemically equivalent Teflon surface.

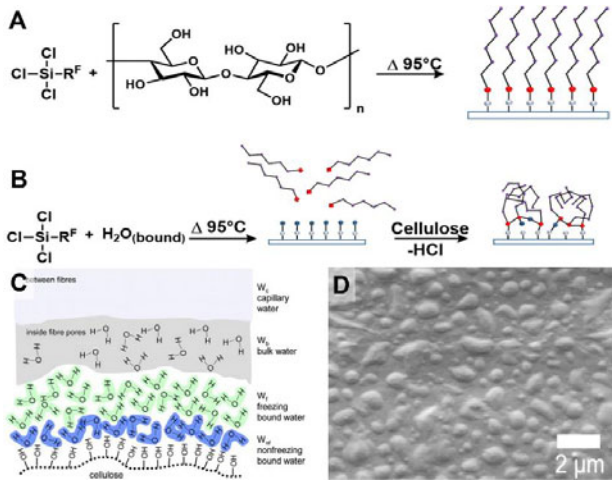

Figure 3. (A) Suggested literature reaction of silanes with cellulose versus (B) proposed bound water reaction (Reproduced from RSC Advances 6, 82233 (2016) with permission of The Royal Society of Chemistry).[53] (C) Diagram of different layers of bound water around cellulose fibers (Reproduced from Carbohydrate Polymers 93, 316 (2013) with permission of Elsevier).[54] (D) Particles formed on paper surface after treatment with silane (Reproduced from Journal of Materials Chemistry A 4, 14729 (2016) with permission of The Royal Society of Chemistry).[17]

Furthermore, thermal degradation of the treated paper showed that no hydrogen fluoride (HF) was released [55] in any detectable amounts, instead a liquid adduct distillate of the silane was obtained.[53] Based on the temperatures at which this distillate was obtained, a depolymerisation process was inferred further supporting the step-growth PISA process.

Fabrication of paper with tunable wetting properties expands their application as functional materials. An important area is the growing use of point-of-care (PoC) devices in developing countries. The lack of dedicated waste streams resulted in their disposition into conventional waste dumps. Individuals who scavenge this waste as a way of life put themselves and their communities at risk.[56] Thus, biodegradable test strips are highly desired for such conditions. Oyola et. al. demonstrated that paper treated with silane could replace the bulky plastic casings. Paper casings have significantly lighter weight and does not interfere with the test procedure. Figure 4A-C illustrates commercial test strip compared to the paper-based device. These fabricated paper-based devices were subsequently buried in an open field to assess natural degradation. Complete degradation of the casing was observed within one year while the plastic had little to no change.[57] Furthermore, the use of paper as a potential structural material has also seen substantial interest, in part due to its adoption in emergency shelter.[58] Chemical treatment of cardboard can be used to extend its lifetime and reduces premature failure due to moisture exposure. Moreover, the treatment of paper surfaces with silanes gives the surface amphiphobic properties, meaning that both hydrophobic and hydrophilic regions exist on the surface.[17] Amphiphobicity is observed as a survival strategy in xeric environments, for example; in the Namib beetle patterned amphiphobicity allows it to harvest water from fog. The hydrophilic regions allow water condensation while hydrophobic regions allow the water to flow into its mouth.[59] This process can be mimicked by creating functional smart surfaces on paper using the step-growth PISA approach (Figure 4D). Felicitous design enables building of an amphiphobic cardboard structure for water harvesting such that moisture condenses from humid air and coalesced droplets collects into a reservoir through a structure and wettability guided flow. Figure 4E-F shows that the treated paper is also useful in its ability to self-clean. Since water does not wet the surface, physisorbed particles can be removed by flowing water on the surface – akin to rain-driven self-cleaning (Figure 4E).[17]

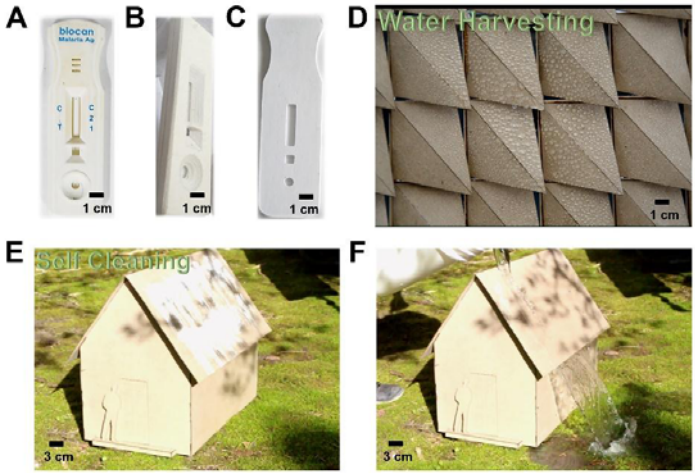

Figure 4. (A-C) Commercially available plastic cased malaria test kit, comparable test kit made of functionalized paper, replica of plastic kit made from treated paper (Reproduced from Industrial Crops and Products 94, 294 (2016) with permission of Elsevier).[57] (D) Water harvesting potential of surface treated cardboard. (E-F) Self-cleaning potential of surface treated cardboard (D-F were reproduced from Journal of Materials Chemistry A 4, 14729 (2016) with permission of The Royal Society of Chemistry).[17]

METASTABILITY: FRUSTRATING THERMODYNAMIC RELAXATION THROUGH INTERFACES

Further understanding of surface reactions coupled with mechanical and chemical approaches to material synthesis can be utilized as a platform to synthesize metastable neoteric materials such as undercooled liquid metal particles. Fluid dynamics (modified emulsification) with concomitant polishing, surface oxidation, and chelation creates stable core shell particle structures.[60] Figure 5A shows a schematic of this top-down particle synthesis method commonly known as SLICE (Shearing liquid into complex particles).[60] This method is an extension of the droplet emulsion technique[61, 62] where liquid metals or metal melts can be converted into 3-layer core-shell particles (Figure 5A insert) of tunable sizes with a passivating oxide layer bearing a compositional gradient.[63] Figure 5B shows the distribution of particle sizes possible ranging from 6 nm to >5 μm. This method has been extended to synthesize, in high-yield, analogous undercooled metal particles by using the core-shell architecture to frustrate solidification.[64]

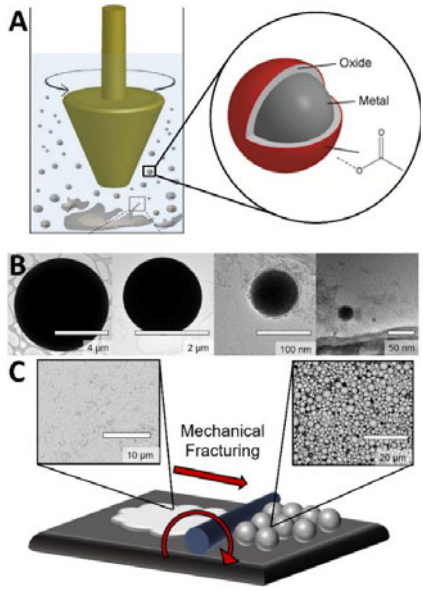

Figure 5. Fabrication and processing of metastable liquid metal particles. (A) Schematic of SLICE particle synthesis technique (Reprinted with permission from Langmuir 30, 14308 (2014). Copyright (2018) American Chemical Society).[60] (B) TEM micrographs showing the spherical and smooth nature of the particles achieved through SLICE. (C) Schematic of mechanical fracturing process.

Undercooled liquids maintain their liquidus state below its melting point (T_m). Solidification can be frustrated either kinetically-where the rates of solidification are extremely low, or thermally- where a large activation energy barrier exists. Concentration gradients at the interface translates to chemical potential gradients ($\Delta\mu$), which could provide such a barrier by significantly altering the free energy landscape. It can be envisioned that nucleation in the bulk only exacerbates the high $\Delta\mu$, hence increased instability. This observation, therefore infers that the interfacial concentration gradients can allow stabilization of otherwise high energy states by frustrating any bulk relaxation.[10] By definition, surfaces and interfaces consist of a limited number of molecules, as such, this chemical potential gradient across two dissimilar entities must be large. This implies that the differences in Gibbs free energy should scale with the concentration gradient. With appropriate design, difference in the Gibbs free energy can be used to frustrate solidification (relaxation) in the system especially when heterogeneous nucleation has already been inhibited by the presence of a stable shell.[65] Since the shell on these particles is fairly thin (nanoscale)[66], hence, unable to isolate the bulk from any significant thermal or mechanical perturbations, relaxation (solidification) can therefore be triggered either by cooling or mechanical deformation.

To maintain undercooling in a metal, heterogeneous nucleation must be eliminated,[67-70] and this is achieved by having a smooth interface (passivating oxide is polished *in situ* during SLICE). It therefore follows that the kinetics of solidification depends on the extent of undercooling, ΔT (eq. 1). Probability of homogeneous

nucleation (I) is, therefore, dependent on ΔT (eq. 1) [10], hence, low-melting alloys can be readily undercooled to ambient using the SLICE particle synthesis approach. N_s is the number of molecules, k is Boltzmann's constant, h is Planck's constant, G is Gibbs free energy, H is enthalpy, γ is surface energy and T_0 is the initial temperature.

$$I = N_s \frac{kT}{h} e^{-\frac{\Delta G_m}{kT}} N e^{-\frac{16\pi\gamma^3 T_0^2}{3(\Delta T)^2(\Delta H_{rxn})^2 kT}} \quad (1)$$

Since the oxide layer is very thin (sub nanometer, ~0.9 nm),[66] it is flexible, hence can offer transient mechanical stability. The protective nature of the oxide layer allows the particles to stack and collide with each other without fracturing. Solidification, however, occurs upon fracturing the oxide layer. This mechanically responsive nature of the undercooled particles can be utilized in ambient condition heat-free soldering. A Low-melting alloy (Field's metal, m.p. = 62°C) was used to demonstrate this capability. Upon shell fracturing the liquid metal flows and solidifies.[64] Figure 5C illustrates particle morphology as it changes from smooth individual spheres into a uniform solidified metal film.

Figure 6A-C shows that the solidification through mechanical fracturing can be used to join two gold films. The solidified Field's metal act as an interlayer between two pieces of gold, creating an interconnect to give Au-FM-Au composite. Furthermore, exploiting asymmetric bonding enables delamination of gold sheet from aluminium foil. Heat-free soldering was also performed to connect two sheets of copper foils (Figure 6D). Resistivity across the fabricated junction compares to that of bulk Field's metal (56 μΩ-cm vs 52 μΩ-cm respectively).[71] This demonstrates that heat-free soldering creates a fully metallic interface irrespective of the previous thermodynamic state of the metal. Furthermore, the application of metastable (undercooled) particles was extended to smart composites by incorporating them into a polymer matrix, producing the so-called Stiffness tuning by thermodynamic relaxation (ST3R) composite (Figure 6E).[72] These composite materials are based on the realization that within each particle, a defined number of atoms are isolated creating a unique closed thermodynamic system. Maxwell-Boltzmann (MB) statistics, therefore, dictates that each particle has a size dependent thermodynamic potential. Considering a stochastic distribution in the sizes, hence thermodynamic potential, stimuli-driven relaxation is expected to follow this Gaussian distribution in size and thermodynamic potential and as dictated by MB statistics. This stochastic behaviour manifested as a change in stiffness of the composite, whereby a shift in skewness of the distribution towards higher stiffness was observed.[72] Mechanical deformation of the composite induces solidification of the liquid metal undercooled particles in a tunable manner. This resulted in significant increase in stiffness (300%), which was attributed to solidification of the liquid metal and formation of networks between initially separated particles (Figure 6F). The ST3R composite can be further reconfigured into complex shapes after melting the metal fillers (Figure 6G-H).

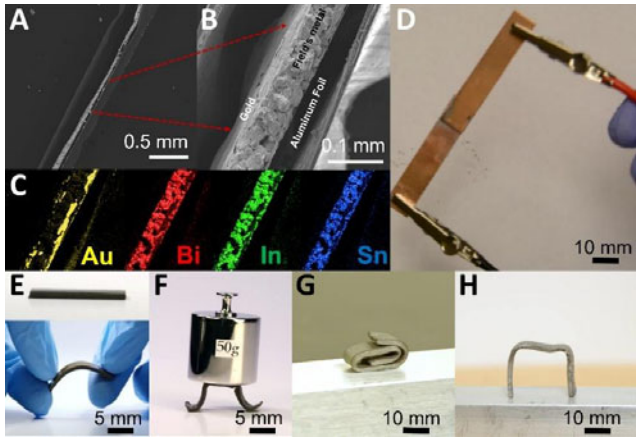

Figure 6. Application of fracturing metastable particles for joining. (A-B) Image of a joined gold sheets by Field`s metal particles. (C) Elemental EDS maps shows the distribution of materials in (B). EDS Detector is positioned on the top right; thus, gold is not apparent on the left side of the sample. (D) Heat-free soldering of copper foils (A-D were reproduced from Sci. Rep., 2016, 6, 21864 with permission from Springer Nature).[21] (E) Metastable particles incorporated into polymer matrix known as the Stiffness tuning by thermodynamic relaxation (ST3R) composite. (F) Stiffness increased by 300%. (G-H) ST3R composite reshaped by melting the metal filler (E-H were reproduced from Mater. Horiz., 2018, Advance Article (DOI: 10.1039/c8mh00032h) with permission of The Royal Society of Chemistry).[72]

CONCLUSION

In conclusion, we demonstrate that understanding the structure, chemistry and thermodynamics of surfaces and interfaces allows one to tune material properties and fabricate functional materials. Self-assembled monolayers (SAM) significantly change the wetting properties of surfaces. Structural changes such as substrate morphology and conformational defects, however, controls the observed wettability. Physisorbed water on the surfaces of cellulose was utilized to perform step-growth polymerization, and subsequent fabrication of amphiphobic paper. This modified paper can be used as a structural material and in water harvesting due to its unique amphiphobicity. Finally, through appropriate design of liquid metal and oxide interface, we navigate around the thermodynamic energy landscape of molten metal to frustrate solidification hence synthesize ambient undercooled liquid metal particles. We demonstrate that these metastable systems can be used as heat-free solders, in fabrication of metal-metal hetero-structures, and incorporated in polymers to produce smart composites. These three case studies illustrate the versatility of surfaces and interfaces in material processing, realizing new uses of well-known materials or creating neoteric functional materials.

References

[1] Merriam-Webster Dictionary, (Merriam-Webster 2018).
[2] H.Y. Erbil: Surface chemistry of solid and liquid interfaces, (Wiley Online Library 2006).
[3] B. Jamtveit and P. Meakin: Growth, dissolution and pattern formation in geosystems, in Growth, Dissolution and Pattern Formation in Geosystems (Springer1999), pp. 1.
[4] C. Ciracì, R. Hill, J. Mock, Y. Urzhumov, A. Fernández-Domínguez, S. Maier, J. Pendry, A. Chilkoti and D. Smith. *Science* **337**, 1072 (2012). DOI: 10.1126/science.1224823
[5] J.N. Anker, W.P. Hall, O. Lyandres, N.C. Shah, J. Zhao and R.P. Van Duyne. *Nat Mater* **7**, 442 (2008). DOI: 10.1038/nmat2162
[6] R. Maboudian and C. Carraro. *Annu. Rev. Phys. Chem.* **55**, 35 (2004). DOI: 10.1146/annurev.physchem.55.091602.094445
[7] J.J. Gooding and D.B. Hibbert. *TrAC Trends in Analytical Chemistry* **18**, 525 (1999). DOI: 10.1016/S0165-9936(99)00133-8
[8] S. Oyola-Reynoso, A.P. Heim, J. Halbertsma-Black, C. Zhao, I.D. Tevis, S. Çınar, R. Cademartiri, X. Liu, J.-F. Bloch and M.M. Thuo. *Talanta* **144**, 289 (2015). DOI: 10.1016/j.talanta.2015.06.018
[9] Z. Wang, J. Chen, S.M. Gathiaka, S. Oyola-Reynoso and M. Thuo. *Langmuir* **32**, 10358 (2016). DOI: 10.1021/acs.langmuir.6b01681
[10] R. DeHoff: Thermodynamics in materials science, (CRC Press2006).
[11] R. Alert, J. Casademunt and P. Tierno. *Physical review letters* **113**, 198301 (2014). DOI: 10.1103/PhysRevLett.113.198301
[12] R. Alert, P. Tierno and J. Casademunt. *Nature communications* **7**, 13067 (2016). DOI: 10.1038/ncomms13067
[13] B. Arkles. *Chemtech* **7**, 766 (1977). DOI: N/A
[14] R. Maoz, J. Sagiv, D. Degenhardt, H. Möhwald and P. Quint. *Supramolecular Science* **2**, 9 (1995). DOI: 10.1016/0968-5677(96)85635-5
[15] V.V. Naik, R. Städler and N.D. Spencer. *Langmuir* **30**, 14824 (2014). DOI: 10.1021/la503739j
[16] H.-G. Steinrück, J. Will, A. Magerl and B. Ocko. *Langmuir* **31**, 11774 (2015). DOI: 10.1021/acs.langmuir.5b03091
[17] S. Oyola-Reynoso, I. Tevis, J. Chen, B. Chang, S. Çinar, J.-F. Bloch and M. Thuo. *Journal of Materials Chemistry A* **4**, 14729 (2016). DOI: 10.1039/C6TA06446A
[18] J. Chen, Z. Wang, S. Oyola-Reynoso and M.M. Thuo. *Langmuir* **33**, 13451 (2017). DOI: 10.1021/acs.langmuir.7b01937
[19] A.M. Russell: Structure-property relations in nonferrous metals, (Hoboken, NJ : John Wiley, Hoboken, NJ, 2005).
[20] C.-T. Sah, R.N. Noyce and W. Shockley. *Proceedings of the IRE* **45**, 1228 (1957). DOI:
[21] S. Çınar, I.D. Tevis, J. Chen and M. Thuo. *Scientific Reports* **6**, 21864 (2016). DOI: 10.1038/srep21864
[22] J. Chen, Z. Wang, S. Oyola-Reynoso, S.M. Gathiaka and M. Thuo. *Langmuir* **31**, 7047 (2015). DOI: 10.1021/acs.langmuir.5b01662
[23] R.N. Sodhi, P. Brodersen, L. Cademartiri, M.M. Thuo and C.A. Nijhuis. *Surface and Interface Analysis* **49**, 1309 (2017). DOI:
[24] Z.J. Farrell and C. Tabor. *Langmuir* **34**, 234 (2018). DOI: 10.1021/acs.langmuir.7b03384
[25] M. Dumke, T. Tombrello, R. Weller, R. Housley and E. Cirlin. *Surface Science* **124**, 407 (1983). DOI: 10.1016/0039-6028(83)90800-2
[26] M. Regan, P.S. Pershan, O. Magnussen, B. Ocko, M. Deutsch and L. Berman. *Physical Review B* **55**, 15874 (1997). DOI: 10.1103/PhysRevB.55.15874
[27] H. Tostmann, E. DiMasi, B. Ocko, M. Deutsch and P.S. Pershan. *Journal of non-crystalline solids* **250**, 182 (1999). DOI: 10.1016/S0022-3093(99)00226-4
[28] L.B. Newcomb, I. Tevis, M.B. Atkinson, S.M. Gathiaka, R.E. Luna and M.M. Thuo. *Langmuir* **30**, 11985 (2014). DOI: 10.1021/la5032569
[29] Z. Wang, J. Chen, S. Oyola-Reynoso and M. Thuo. *Langmuir* **32**, 8230 (2016). DOI: 10.1021/acs.langmuir.6b02159
[30] Z. Wang, J. Chen, S. Oyola-Reynoso and M. Thuo. *Coatings* **5**, 1034 (2015). DOI: 10.3390/coatings5041034
[31] M.M. Thuo, W.F. Reus, C.A. Nijhuis, J.R. Barber, C. Kim, M.D. Schulz and G.M. Whitesides. *Journal of the American Chemical Society* **133**, 2962 (2011). DOI: 10.1021/ja1090436
[32] D.M. Walba, C.A. Liberko, E. Korblova, M. Farrow, T.E. Furtak, B.C. Chow, D.K. Schwartz, A.S. Freeman, K. Douglas and S.D. Williams. *Liquid Crystals* **31**, 481 (2004). DOI: 10.1080/02678290410001666075
[33] R.J. Kline, M.D. McGehee and M.F. Toney. *Nature Materials* **5**, 222 (2006). DOI: 10.1038/nmat1590
[34] L. Jiang, C.S. Sangeeth and C.A. Nijhuis. *Journal of the American Chemical Society* **137**, 10659 (2015). DOI: 10.1021/jacs.5b05761
[35] J. Chen, B. Chang, S. Oyola-Reynoso, Z. Wang and M. Thuo. *ACS Omega* **2**, 2072 (2017). DOI: 10.1021/acsomega.7b00355
[36] Y. Yang, A.C. Jamison, D. Barriet, T.R. Lee and M. Ruths. *Journal of Adhesion Science and Technology* **24**, 2511 (2010). DOI: 10.1163/016942410X508253
[37] L. Ramin and A. Jabbarzadeh. *Langmuir* **28**, 4102 (2012). DOI: 10.1021/la204701z

[38] J. Chen, J. Liu, I.D. Tevis, R.S. Andino, C.M. Miller, L.D. Ziegler, X. Chen and M.M. Thuo. *Physical Chemistry Chemical Physics* **19**, 6989 (2017). DOI: 10.1039/C6CP07580K
[39] N. Nishi, D. Hobara, M. Yamamoto and T. Kakiuchi. *The Journal of chemical physics* **118**, 1904 (2003). DOI: 10.1063/1.1531098
[40] P. Cyganik, K. Szelagowska-Kunstman, A. Terfort and M. Zharnikov. *The Journal of Physical Chemistry C* **112**, 15466 (2008). DOI: 10.1021/jp805303r
[41] K. Heister, H.-T. Rong, M. Buck, M. Zharnikov, M. Grunze and L. Johansson. *The Journal of Physical Chemistry B* **105**, 6888 (2001). DOI: 10.1021/jp010180e
[42] F. Chesneau, B. Schüpbach, K. Szelągowska-Kunstman, N. Ballav, P. Cyganik, A. Terfort and M. Zharnikov. *Physical Chemistry Chemical Physics* **12**, 12123 (2010). DOI: 10.1039/C0CP00317D
[43] M. Zharnikov. *Journal of Electron Spectroscopy and Related Phenomena* **178**, 380 (2010). DOI: 10.1016/j.elspec.2009.05.008
[44] L. Ramin and A. Jabbarzadeh. *Langmuir* **27**, 9748 (2011). DOI: 10.1021/la201467b
[45] A.A. Craig and C.T. Imrie. *Macromolecules* **28**, 3617 (1995). DOI: 10.1021/ma00114a015
[46] L. Ramin and A. Jabbarzadeh. *Modelling and Simulation in Materials Science and Engineering* **20**, 085010 (2012). DOI: 10.1088/0965-0393/20/8/085010
[47] A.T. Marcelis, A. Koudijs and E.J. Sudhölter. *Thin Solid Films* **284**, 308 (1996). DOI: 10.1016/S0040-6090(95)08330-8
[48] A. Yamaguchi, M. Watanabe and A. Yoshizawa. *Liquid Crystals* **34**, 633 (2007). DOI: 10.1080/02678290701292355
[49] J. Sporrer, J. Chen, Z. Wang and M.M. Thuo. *The Journal of Physical Chemistry Letters* **6**, 4952 (2015). DOI: 10.1021/acs.jpclett.5b02300
[50] C. Frankiewicz and D. Attinger. *Nanoscale* **8**, 3982 (2016). DOI: 10.1039/C5NR04098A
[51] A.C. Glavan, R.V. Martinez, A.B. Subramaniam, H.J. Yoon, R.M.D. Nunes, H. Lange, M.M. Thuo and G.M. Whitesides. *Adv Funct Mater* **24**, 60 (2014). DOI: 10.1002/adfm.201300780
[52] J.G. Matisons: Silane coupling agents and glass fibre surfaces: a perspective, in Silanes and other coupling agents, edited by M. J. Owen, Dvornic, Petar R. (Springer Netherlands, Advances in Silicon Science, 2009), pp. 281.
[53] S. Oyola-Reynoso, J. Chen, B.S. Chang, J.-F. Bloch and M.M. Thuo. *RSC Advances* **6**, 82233 (2016). DOI: 10.1039/C6RA20582H
[54] T. Bechtold, A.P. Manian, H.B. Öztürk, U. Paul, B. Široká, J. Široký, H. Soliman, L.T.T. Vo and H. Vu-Manh. *Carbohydrate Polymers* **93**, 316 (2013). DOI: 10.1016/j.carbpol.2012.01.064
[55] F.L.M. Pattison and R.E.A. Dear. *Can. J. Chem.* **41**, 2600 (1963). DOI: 10.1139/v63-380
[56] J. Otieno: Rising chemical use, lax dumping rules leave Africa choking on waste, in Business Daily (businessdailyafrica.com, 2012), p. 4.
[57] S. Oyola-Reynoso, D. Kihereko, B.S. Chang, J.N. Mwangi, J. Halbertsma-Black, J.-F. Bloch, M.M. Thuo and M.M. Nganga. *Industrial Crops and Products* **94**, 294 (2016). DOI: 10.1016/j.indcrop.2016.08.051
[58] S. Ban and R. Miyake: Shigeru BAn: paper in architecture, (New York: Rizzoli International Publications, New York, 2009).
[59] J. Guadarrama-Cetina, A. Mongruel, M.G. Medici, E. Baquero, A.R. Parker, I. Milimouk-Melnytchuk, W. Gonzalez-Vinas and D. Beysens. *European Physical Journal E: Soft Matter and Biological Physics* **37**, 1 (2014). DOI: 10.1140/epje/i2014-14109-y
[60] I.D. Tevis, L.B. Newcomb and M. Thuo. *Langmuir* **30**, 14308 (2014). DOI: 10.1021/la5035118
[61] Y. Wang and Y. Xia. *Nano Letters* **4**, 2047 (2004). DOI: 10.1021/nl048689j
[62] W.P. Allen and J.H. Perepezko. *Metallurgical Transactions A* **22**, 753 (1991). DOI: 10.1007/BF02670298
[63] L. Cademartiri, M.M. Thuo, C.A. Nijhuis, W.F. Reus, S. Tricard, J.R. Barber, R.N.S. Sodhi, P. Brodersen, C. Kim, R.C. Chiechi and G.M. Whitesides. *The Journal of Physical Chemistry C* **116**, 10848 (2012). DOI: 10.1021/jp212501s
[64] S. Cinar, I.D. Tevis, J. Chen and M. Thuo. *Sci. Rep.* **6**, 21864 (2016). DOI: 10.1038/srep21864
[65] J.H. Perepezko. *Materials Science and Engineering* **65**, 125 (1984). DOI: 10.1016/0025-5416(84)90206-4
[66] I.D. Tevis, L.B. Newcomb and M. Thuo. *Langmuir* **30**, 14308 (2014). DOI: 10.1021/la5035118
[67] D. Herlach: Containerless Undercooling And Solidification Of Pure Metals, (1991).
[68] D. Herlach. *Metals* **4**, 196 (2014). DOI: 10.3390/met4020196
[69] J.H. Perepezko and J.S. Paik. *MRS Online Proceedings Library* **8**, null (1981). DOI: 10.1557/PROC-8-49
[70] J.H. Perepezko, J.L. Sebright, P.G. Höckel and G. Wilde. *Materials Science and Engineering: A* **326**, 144 (2002). DOI: 10.1016/S0921-5093(01)01430-7
[71] M. Kamal, A.-B. El-Bediwi, R. Shalaby and M. Younus. *Journal of Advances in Physics* 1404 (2011). DOI: N/A
[72] B.S. Chang, R. Tutika, J. Cutinho, S. Oyola-Reynoso, J. Chen, M.D. Bartlett and M.M. Thuo. *Mater. Horiz.*, Ahead of Print (2018). DOI: 10.1039/c8mh00032h